

DOI: 10.24425/amm.2021.136364

SEONG-HO HA^{1*}, ABDUL WAHID SHAH¹, BONG-HWAN KIM¹,
YOUNG-OK YOON¹, HYUN-KYU LIM¹, SHAE K. KIM¹

EFFECT OF Cu ADDITION ON OXIDE GROWTH OF Al-7 MASS%Mg ALLOY AT HIGH TEMPERATURE

Effect of Cu addition on oxide growth of Al-7 mass%Mg alloy at high temperature was investigated. As-cast microstructures of Al-7 mass%Mg and Al-7 mass%Mg-1 mass%Cu alloys showed α -Al dendrites and area of secondary particles. The 1 mass%Cu addition into Al-7 mass%Mg alloy formed $Mg_{32}(Al, Cu)_{49}$ ternary phase with β - Al_3Mg_2 . The total fraction of two Mg-containing phases in Cu-added alloy was higher than the β - Al_3Mg_2 fraction in Cu-free alloy. From measured weight gains depending on time at 500°C under an air atmosphere, it was shown that all samples exhibited significant weight gains depending on time. Al-7mass%Mg-1mass%Cu alloy showed the relatively increased oxidation rate when compared with Cu-free alloy. All the oxidized cross-sections throughout the entire oxidation time showed coarse and dark areas regarded as oxides grown from the surface to inside, but bigger oxidized areas were formed in the Al-7mass%Mg-1mass%Cu alloy containing higher fraction of Mg-based phases in the as-cast microstructure. As a result of compositional analysis on the oxide clusters, it was found that the oxide clusters contained Mg-based oxides formed through internal oxidation during a long time exposure to oxidizing environments.

Keywords: Al-Mg system, Cu addition, Oxidation, phase diagram

1. Introduction

For further weight reduction of Al alloys as structural materials, Al-Mg alloys are increasingly used owing to their excellent corrosion resistance, weldability, and formability and the lightweight of Mg as the alloying element [1]. The needs to increase Mg to more than 5 mass% in Al alloys has intensified due to its high tensile and fatigue strength and better weldability. Non-heat treatable Al-Mg alloys have the highest strengths in Al alloys without heat treatment [1]. However, their strengths are limited when compared with those of heat-treatable alloys with proper heat treatments. The addition of third elements can make Al-Mg alloys heat treatable by forming Mg-based phases as strengthening agents. Cu is the main alloying element of 2xxx series Al alloy, some of the highest strength heat treatable Al alloys [1]. Therefore, Cu addition into Al-Mg alloys can provide the improvement of strength. Only a few studies have examined Al-Mg-Cu or Al-Cu-Mg systems containing Mg contents over 1 mass% [2-4]. Watanabe et al. investigated the effect of Cu on superplastic behavior of Al-Mg base alloy (AA5083) whose the Mg content was approximately 5 mass% [2]. The strengthening mechanisms and precipitation behavior of AA2024 alloys

with different Cu/Mg ratios were studied by García-Hernández et al. [3]. Mihara et al. also examined the precipitation of Al-3 mass%Mg-1 mass%Cu based alloys [4]. The Mg contents considered in the previous studies aforementioned have been below 5 mass%, which is considered as a critical Mg content to maintain relatively low oxidation rates of Al-Mg alloys [5]. No studies have examined the oxidation behaviors of Al-Mg-Cu or Al-Cu-Mg alloys containing high contents of Mg.

In Al-Mg alloys, Mg enrichment increases oxidation tendency of the alloys at elevated temperatures for the heat treatments [5-7]. Al-Mg binary system forms β - Al_3Mg_2 phase by eutectic reaction during solidification [8]. Such a highly Mg-enriched phase at grain boundaries is preferentially oxidized and strongly affects the oxidation behavior of matrix at high temperatures. The oxidation of β - Al_3Mg_2 phase can lead to a continuous oxidation along the grain boundaries. The Al-Cu-Mg alloys form Al_2CuMg , a ternary strengthening phase [9]. The co-existence of β - Al_3Mg_2 and Al_2CuMg phases at grain boundaries can change the oxidation behavior. The aim of this study is to investigate effect of Cu addition on oxide growth of Al-7 mass%Mg alloy at high temperature. The correlation between oxidation resistance and phase fractions of Mg-based intermetallic compounds was discussed.

¹ KOREA INSTITUTE OF INDUSTRIAL TECHNOLOGY (KITECH), ADVANCED MATERIALS AND PROCESS R&D DEPARTMENT, INCHEON 21999, REPUBLIC OF KOREA

* Corresponding author: seonghoha1999@gmail.com



2. Experimental

Composition of the alloy examined in this study is Al-7 mass%Mg, whose the Mg content is in the composition range of 535 Al alloy, one of commercially used Al-Mg casting alloys [1]. Alloys were made in an induction furnace under ambient atmosphere. Pure Al was melted in a graphite crucible at 750°C and then, 7 mass%Mg in the form of pure Mg ingot was added into the melt. Then, 1 mass% of Cu in the form of Al-50 mass%Cu master alloy was added for the Cu added alloy. After that, each alloy melt was cast into a steel mold that was preheated to 200°C. As-cast microstructures were observed using optical microscope after etching the surface of polished samples with Keller's reagent. Isothermal oxidation tests were carried out by thermal gravimetric analysis (TGA, TA Instruments SDT-Q600) under an air atmosphere at 500°C, which is in the temperature ranges of solution heat treatments for Al alloys [1]. Cross-sections of oxidized surfaces formed on the samples were observed and analyzed using field emission (FE) – scanning electron microscopy (SEM, FEI Quanta

200 FEG) equipped with an energy dispersive X-ray spectroscopy (EDS) detector. Phase fractions in the as-cast alloys were predicted on the basis of calculations of Scheil-Gulliver cooling by *FactSage 7.3* [10]. Phase equilibria between each alloy and O₂ were also calculated by *FactSage 7.3* to predict the possible oxide formations at aforementioned oxidation conditions.

3. Results and discussion

Fig. 1 represents the as-cast microstructures of all examined Al-7mass%Mg-based alloys. Each as-cast microstructure includes α -Al dendrites and area of secondary particles. There is no significant change in the microstructures between Al-7 mass%Mg and Al-7 mass%Mg-1 mass%Cu alloys. However, 1 mass%Cu added alloy seems to have relatively uniform distribution of eutectic phases. The cooling curves and phase fraction of alloys examined in the study after Scheil-Gulliver coolings calculated by *FactSage 7.3* are shown in Fig. 2. Only

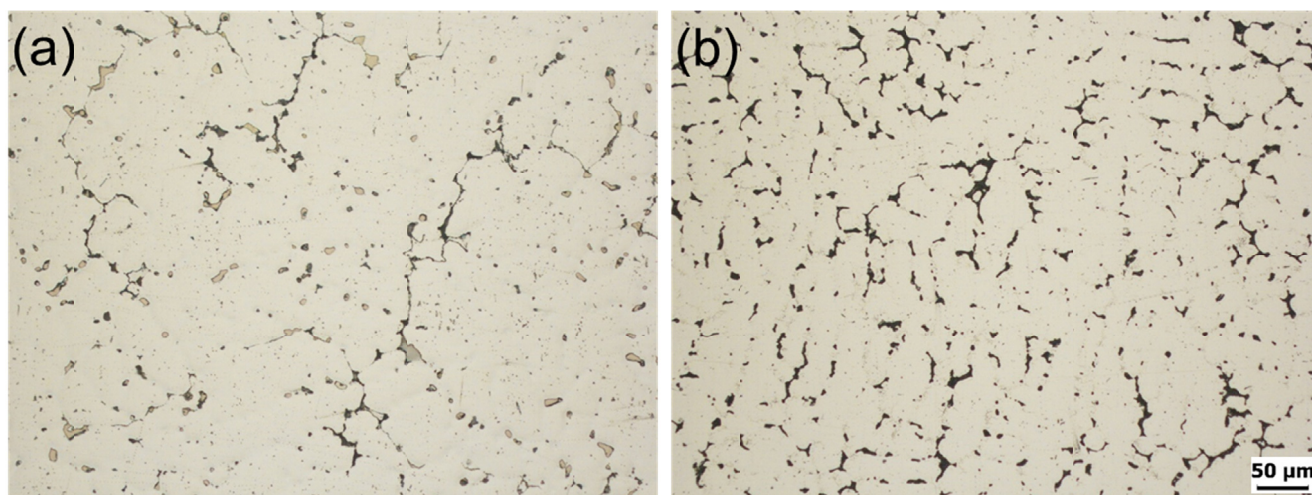


Fig. 1. Optical microstructures of as-cast alloys. (a) Al-7 mass%Mg and (b) Al-7 mass%Mg-1 mass%Cu alloys

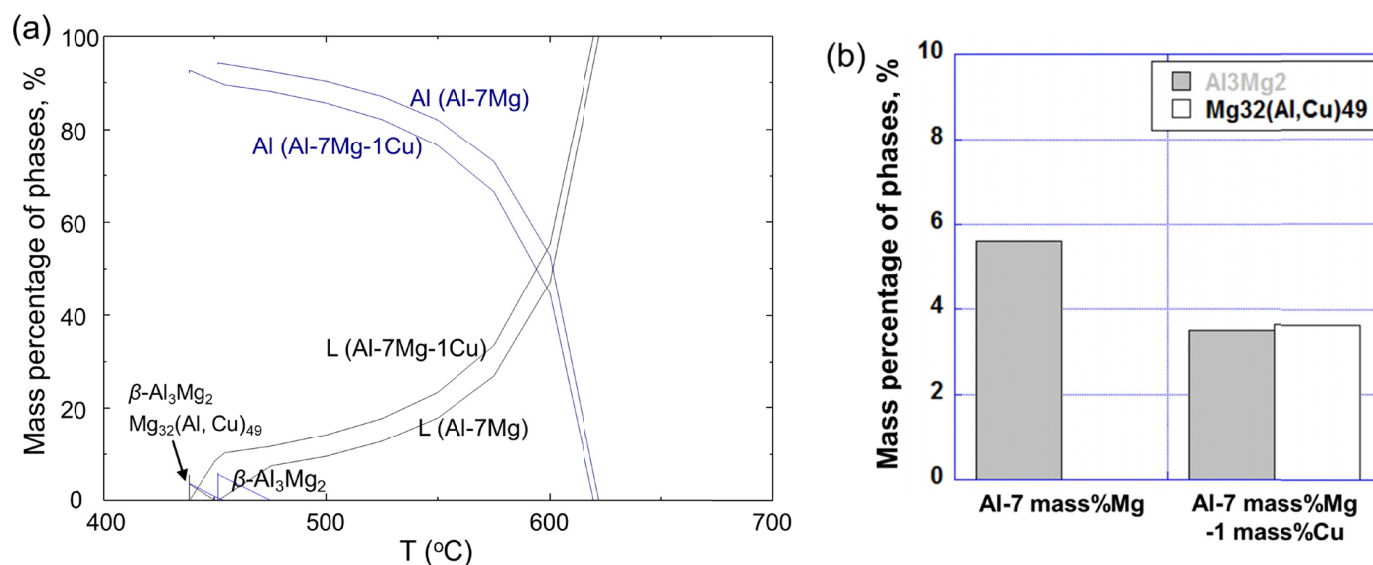


Fig. 2. (a) Scheil-Gulliver cooling curves and (b) secondary phase fractions of examined alloys calculated by *FactSage 7.3*

difference in eutectic phase formation is that the 1mass%Cu addition into Al-7 mass%Mg alloy forms $Mg_{32}(Al, Cu)_{49}$ ternary phase with $\beta-Al_3Mg_2$. And also, Al-7 mass%Mg-1 mass%Cu alloy shows the cooling curves with lower temperatures. The fraction of $\beta-Al_3Mg_2$ in Cu-free alloy is higher than that in Cu-added alloy, while the total fraction of two Mg-containing phases in Cu-added alloy is higher than the $\beta-Al_3Mg_2$ fraction in Cu-free alloy.

Fig. 3 shows the measured weight gains of the examined alloys depending on time at 500°C under an air atmosphere. All samples exhibited significant weight gains depending on time. The mass gain of Cu-free alloy sample appears to possess relatively lower rates and follow nearly linear laws. In the Al-7 mass%Mg-1 mass%Cu alloy sample, a weight gain, which follows the parabolic law, was found after approximately 50 min. The increased oxidation rate in the Al-7mass%Mg-1mass%Cu alloy can be related to higher total fraction of Mg-containing phases.

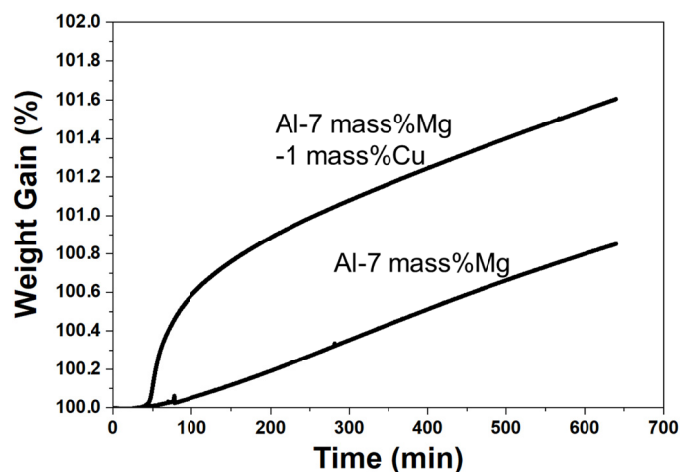


Fig. 3. Weight gains of examined alloys depending on time at 500°C under a dry air atmosphere

Fig. 4 displays SEM-backscattered electron (BSE) images of the cross-sections oxidized at 500°C. All the oxidized cross-sections throughout the entire oxidation time show coarse and dark areas grown from the surface to inside, but no uniformly thickened outermost oxide layers. Since the elements with higher atomic numbers backscatter electrons more strongly than those with lower atomic numbers, the dark areas are considered as Mg-based oxides. The noticeable thing is that bigger oxidized areas are formed in the Al-7mass%Mg-1mass%Cu alloy containing higher fraction of Mg-based phases in the as-cast microstructure. And also, it is worth noting that a number of fine particles are distributed near the surface of Al-7mass%Mg alloy.

Compositional analysis of the numbered areas shown in Fig. 4 by SEM-EDS is given in Table 1. From the compositions for the dark areas, it is found that the oxide clusters containing Mg-based oxides are formed through internal oxidation during a long time exposure to oxidizing environments. The matrix surrounding the oxide clusters such as 5 has the significantly reduced Mg contents. It is considered that the Mg consumption by the growth of Mg based oxides following oxygen diffusion inside led to the reduction of Mg content in the matrix near the oxide clusters. The fine particles numbered as 2 and 6 are relatively Mg-enriched without oxygen. This may be attributed

TABLE 1

Compositional analysis of areas shown in Fig. 4 by SEM-EDS

Area	Analyzed composition (mass%)		
	Al	Mg	O
1	11.16	62.29	26.56
2	94.88	5.12	—
3	33.72	46.20	20.08
4	4.08	70.57	25.34
5	98.33	1.67	6.50
6	94.13	5.87	—

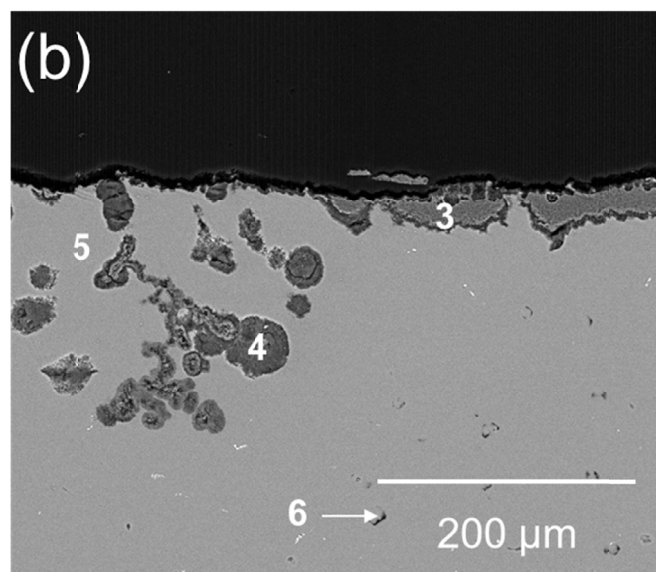
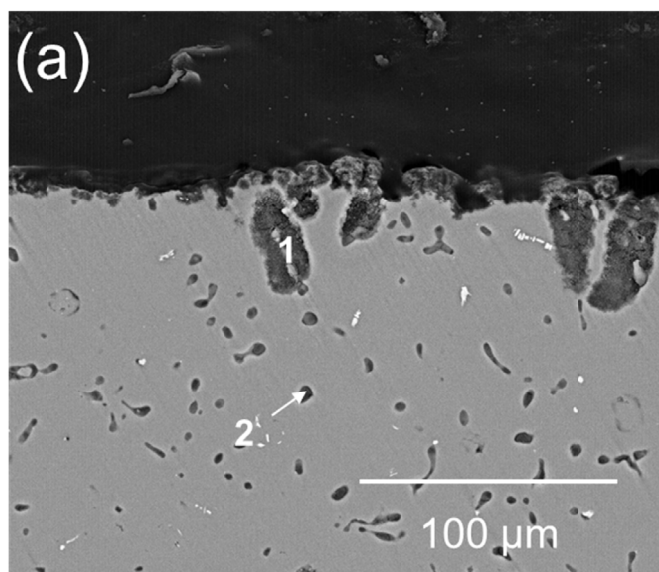


Fig. 4. SEM-backscattered electron (BSE) image of cross-sections oxidized at 500°C for 15 h. (a) Al-7 mass%Mg and (b) Al-7 mass%Mg-1 mass%Cu alloys

to the precipitations from surface enrichment of Mg during the oxidation. However, Al-7 mass%Mg-1 mass%Cu alloy has the distribution of much less particles. A greater amount of Mg was possibly consumed, leading to more significant Mg-based oxide formation. And also, no Cu was detected in the oxide layers, indicating that the addition of 1 mass%Cu rarely produced Cu-based oxides. The two main oxides which cause the growth of oxide layer on the surfaces of Al-Mg alloys were reported to be MgO and $MgAl_2O_4$ -spinel according to previous reports [11,12]. Therefore, it was thought that the oxide layers and clusters were comprised of MgO and spinel.

Phase equilibria between Mg-based intermetallics and O_2 at 500°C calculated by *FactSage 7.3* are shown in Fig. 5. These results indicate that the MgO is the first formed oxide in both cases by the interaction with oxygen as O_2 fraction increases. After a great consumption of Mg in the phases, spinel is formed following the further increase of O_2 fraction. $Mg_{32}(Al, Cu)_{49}$ ternary phase and $\beta-Al_3Mg_2$ show a similar oxide formation at the same condition. Therefore, the oxidation tendency in the two examined alloys would be more likely to dependent on the total fraction of Mg-based phases. The higher fraction of Mg-based phases in Al-7mass%Mg-1mass%Cu alloy might be subject to a selective oxidation and trigger the growth rate of oxide clusters.

4. Conclusions

As-cast microstructures of Al-7 mass%Mg and Al-7 mass%Mg-1 mass%Cu alloys showed α -Al dendrites and area of secondary particles. Al-7 mass%Mg-1 mass%Cu alloy included $Mg_{32}(Al, Cu)_{49}$ ternary phase and $\beta-Al_3Mg_2$ as the secondary phases. The total fraction of two Mg-containing phases in Cu-added alloy was higher than the $\beta-Al_3Mg_2$ fraction in Cu-free alloy. As a result of weight gains by TGA depending on time at 500°C under an air atmosphere, all samples exhibited significant weight gains depending on time. Al-7mass%Mg-1mass%Cu alloy showed the relatively higher oxidation rate when compared with Cu-free alloy. All the oxidized cross-sections showed coarse and dark areas considered as oxides grown from the surface to inside, but bigger oxidized areas were formed in the Al-7mass%Mg-1mass%Cu alloy containing higher fraction of Mg-based phases in the as-cast microstructure. From compositional analysis on the oxide clusters, it was found that the oxide clusters contained Mg-based oxides formed through internal oxidation during a long duration. The higher fraction of Mg-based phases in Al-7mass%Mg-1mass%Cu alloy might be subject to a selective oxidation and accelerate the growth of oxide clusters.

Acknowledgments

This work was supported by funding (No. 20011420) from Ministry of Trade, Industry and Energy, Korea.

REFERENCES

- [1] J.R. Davis, ASM International, Aluminum and Aluminum Alloys, Materials Park 1993.
- [2] H. Watanabe, K. Ohori, Y. Takeuchi, Trans. Iron Steel Inst. Jpn. **27**, 730 (1987).
- [3] J.L. García-Hernández, C.G. Garay-Reyes, I.K. Gómez-Barraza, M.A. Ruiz-Esparza-Rodríguez, E.J. Gutiérrez-Castañeda, I. Estrada-Guel, M.C. Maldonado-Orozco, R. Martínez-Sánchez, J. Mater. Res. Technol. **8** (6), 5471 (2019).
- [4] M. Mihara, C.D. Marioara, S.J. Andersen, R. Holmestad, E. Kobayashi, T. Sato, Mater. Sci. Eng. A, **658**, 91 (2016).
- [5] S.H. Ha, B.H. Kim, Y.O. Yoon, H.K. Lim, T.W. Lee, S.H. Lim, S.K. Kim, Int. J. Metalcast. **13**, 121 (2019).
- [6] G. Wu, K. Dash, M.L. Galano, K.A.Q. O'Reilly, Corros. Sci. **155**, 97 (2019).
- [7] B.H. Kim, S.H. Ha, Y.O. Yoon, H.K. Lim, S.K. Kim, D.H. Kim, Mater. Lett. **228**, 108 (2018).
- [8] H. Okamoto, J. Phase Equilibria **19**, 598 (1998).
- [9] T.S. Parel, S.C. Wang, M. J. Starink, Mater. Des. **31**, S2 (2010).
- [10] C.W. Bale, E. Bélisle, P. Chartrand, S.A. Deckerov, G. Eriksson, A.E. Gheribi, K. Hack, I.H. Jung, Y.B. Kang, J. Melançon, A.D. Pelton, S. Petersen, C. Robelin, J. Sangster, P. Spencer, M.A. Van Ende, Calphad **54**, 35 (2016).
- [11] S.H. Ha, B.H. Kim, Y.O. Yoon, H.K. Lim, T.W. Lee, S.H. Lim, S.K. Kim, Sci. Adv. Mater. **10**, 697 (2018).
- [12] D. Ajmera, E. Panda, Corros. Sci. **102**, 425 (2016).

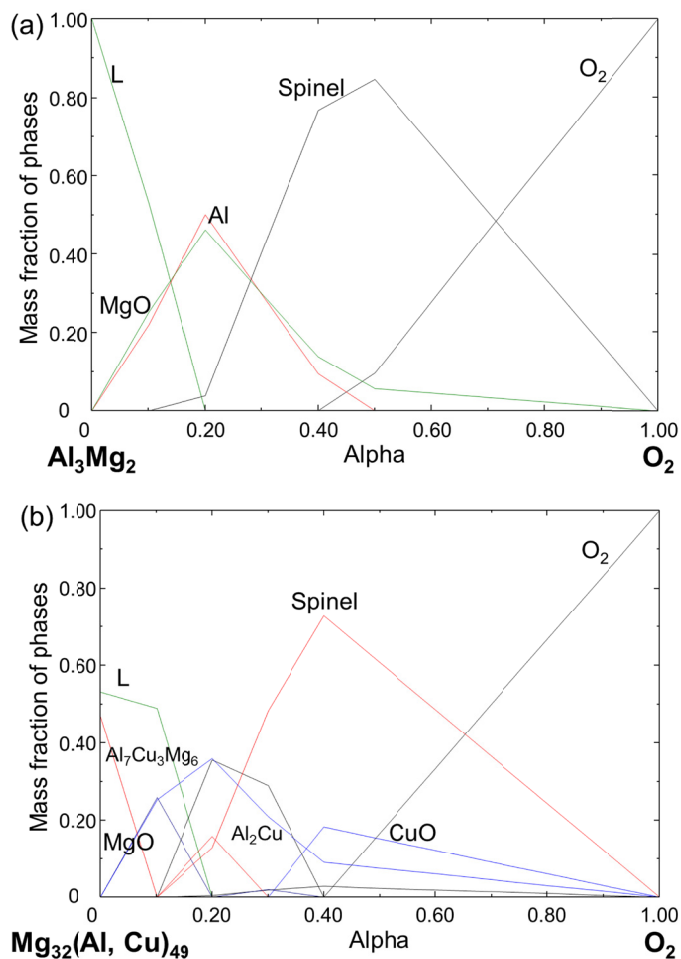


Fig. 5. Phase equilibria between (a) Al_3Mg_2 and O_2 and (b) $Mg_{32}(Al, Cu)_{49}$ and O_2 at 500°C calculated by *FactSage 7.3*